

# GaSb grass as a novel antireflective surface for infrared detectors

Brian J. Pepper, Karl Y. Yee, Alex Soibel, Anita M. Fisher, Sam A. Keo, Arezou Khoshakhlagh, and Sarath D. Gunapala

Center for Infrared Photodetectors, Jet Propulsion Laboratory, California Institute of Technology, 4800 Oak Grove Dr., Pasadena, California 91030, USA

## ABSTRACT

GaSb has a high numerical index (approximately 3.90 at a wavelength of 2  $\mu\text{m}$ ), leading to reflection of about 35% of incoming photons, depending on wavelength. This results in a significant loss of quantum efficiency for GaSb-based infrared detectors when backside-illuminated, since GaSb is the first material encountered. Here we demonstrate a way of etching broadband antireflective GaSb grass using an inductively coupled  $\text{Cl}_2$  plasma etch with  $\text{O}_2$  micromasking, and we examine the possibility for using this material as an antireflective surface for infrared detectors (a patent is pending concerning integration with GaSb-based infrared detectors). We demonstrate sub-10% reflectivity for wavelengths ranging from 200 nm to 12.2  $\mu\text{m}$  and at angles of incidence up to 58°.

**Keywords:** GaSb, black, grass, antireflective, broadband, infrared

## 1. INTRODUCTION

Gallium antimonide (GaSb) is a common wafer material in infrared detectors, such as bulk InAsSb nBn detectors,<sup>1</sup> High Operating Temperature Barrier Infrared Detectors (HOT-BIRDs),<sup>2,3</sup> and other nBn and XBn detectors more broadly.<sup>4,5</sup> However, GaSb has a high numerical index (approximately 3.90 at a wavelength of 2  $\mu\text{m}$ ), leading to reflection of about 35% of incoming photons, depending on wavelength. This causes a loss of quantum efficiency for infrared detectors as GaSb is the first material encountered by incoming photons.

Here we demonstrate a method of etching broadband antireflective GaSb grass using an inductively coupled  $\text{Cl}_2$  plasma etch with  $\text{O}_2$  micromasking. We demonstrate broadband antireflection with sub-10% reflectivity for wavelengths ranging from 200 nm to 12.2  $\mu\text{m}$  (nearly 6 octaves) and at angles of incidence up to 58°. We consider the possibility of using such GaSb grass as an antireflective surface on GaSb-based infrared detectors (a patent is pending regarding this integration). This has several potential advantages over more traditional dielectric coatings. First, we have demonstrated nearly 6 octaves of bandwidth, while typical broadband dielectric coatings are limited to about 2 octaves. Second, we have demonstrated angles of incidence up to 58°, while typical dielectric coatings are limited to angles of incidence of about 45°. Third, since GaSb grass is not a different material deposited on top of the GaSb, it cannot delaminate, as some dielectric coatings do with thermal cycling. Finally, it has potential cost advantages due to the simplicity of the etch.

## 2. PRIOR WORK

Black silicon is a technique of etching nanostructured grass onto silicon wafers by various means.<sup>6–8</sup> Black silicon is mature and widely used for applications such as antireflection on photodetectors, stray light absorption, and coronagraphs.<sup>9,10</sup> Black silicon has demonstrated antireflectivity to wavelengths of many tens of  $\mu\text{m}$  and to angles of incidence as high as 70°.

In addition, several prior works extend this to GaSb and consider nanostructured grass on GaSb or “black GaSb.” Initial works regard it as a nuisance and primarily consider how to avoid it.<sup>11,12</sup> One work involves fabrication using an electron beam mask and fast atom beam  $\text{SF}_6/\text{Cl}_2$  etching, achieving antireflection to 2.3  $\mu\text{m}$ .<sup>13</sup>

---

E-mail: Brian.J.Pepper@jpl.nasa.gov

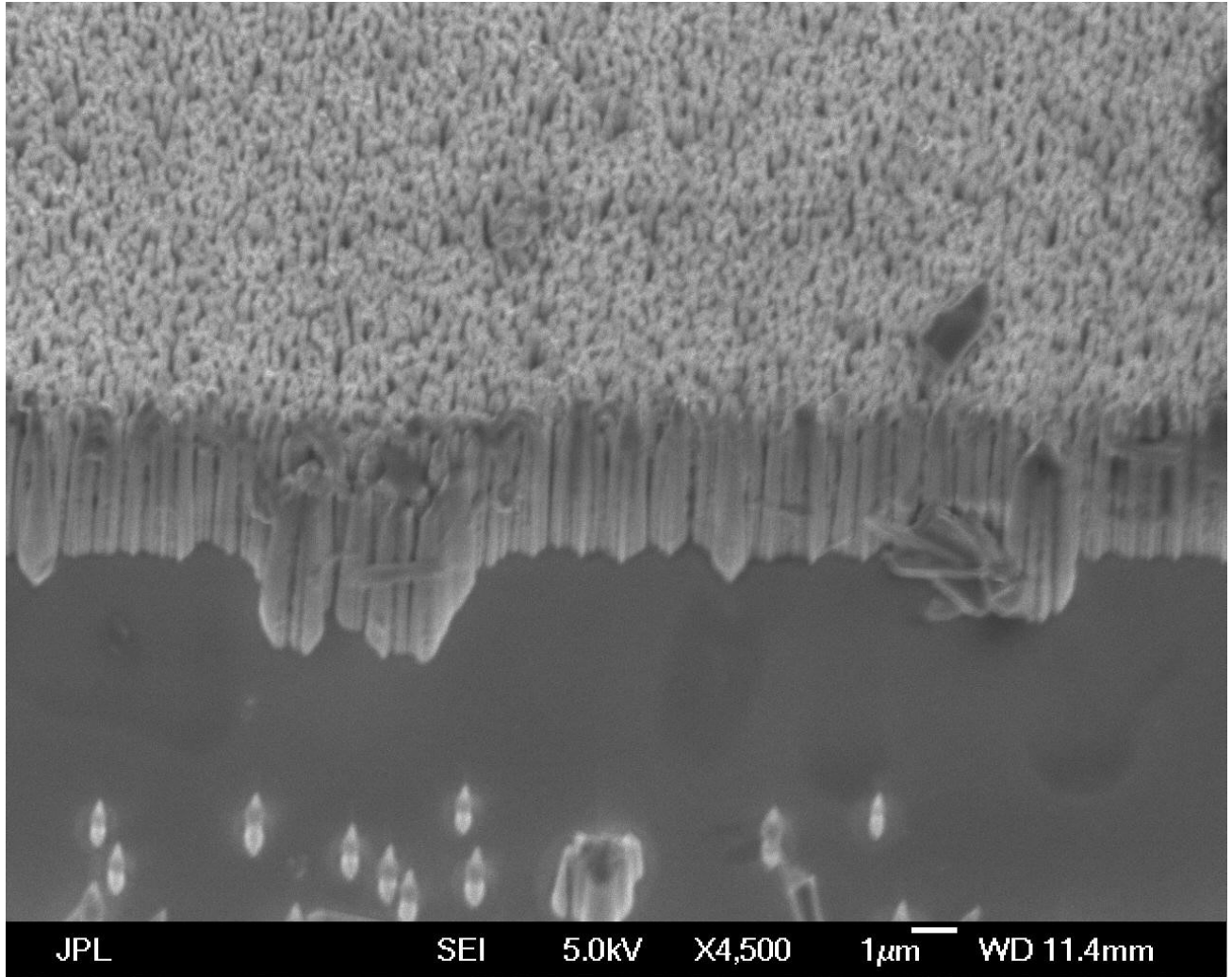


Figure 1. An example scanning electron microscope (SEM) image of GaSb grass produced in this work. The image shows grass of heights approximately 5 to 6  $\mu\text{m}$  and widths approximately 200 to 300 nm. (Note that the sample is viewed at  $30^\circ$  off-normal incidence, causing the heights to appear shorter by half).

Another work uses a silica colloidal array as a mask with a  $\text{Cl}_2$  ICP etch, achieving antireflection to 1.7  $\mu\text{m}$ .<sup>14</sup> Another work uses a  $\text{BCl}_3/\text{O}_2$  and a  $\text{Cl}_2/\text{O}_2$  ICP etch, with the  $\text{O}_2$  causing random micromasking, primarily focusing on nanopillar/nanowire applications but also demonstrating antireflection to 2.0  $\mu\text{m}$ .<sup>15</sup> Finally, another set of works uses  $\text{Ar}^+$  ion irradiation to create nanoporous GaSb, achieving antireflection to 800 nm.<sup>16,17</sup>

The principle on which these nanostructured surfaces work has been considered theoretically<sup>18</sup> and varies somewhat depending on the dimensions of the grass and the wavelength of the light. In the long wavelength regime, with wavelength much larger than the width of the grass, the grass acts like an effective graded index material and prevents reflection by the presence of a slow adiabatic transition in index (this breaks down when wavelength begins to rival the height of the grass, and the transition is no longer so slow or adiabatic). In the short wavelength regime, with wavelength much smaller than the width of the grass, the matter becomes a geometric optics problem, and grass is treated as a “forest” which it is difficult for the light to reflect out of. In the intermediate wavelength regime, however, neither of these pictures is true and full finite difference time domain (FDTD) simulations of Maxwell’s equations are necessary (though the antireflection generally persists).

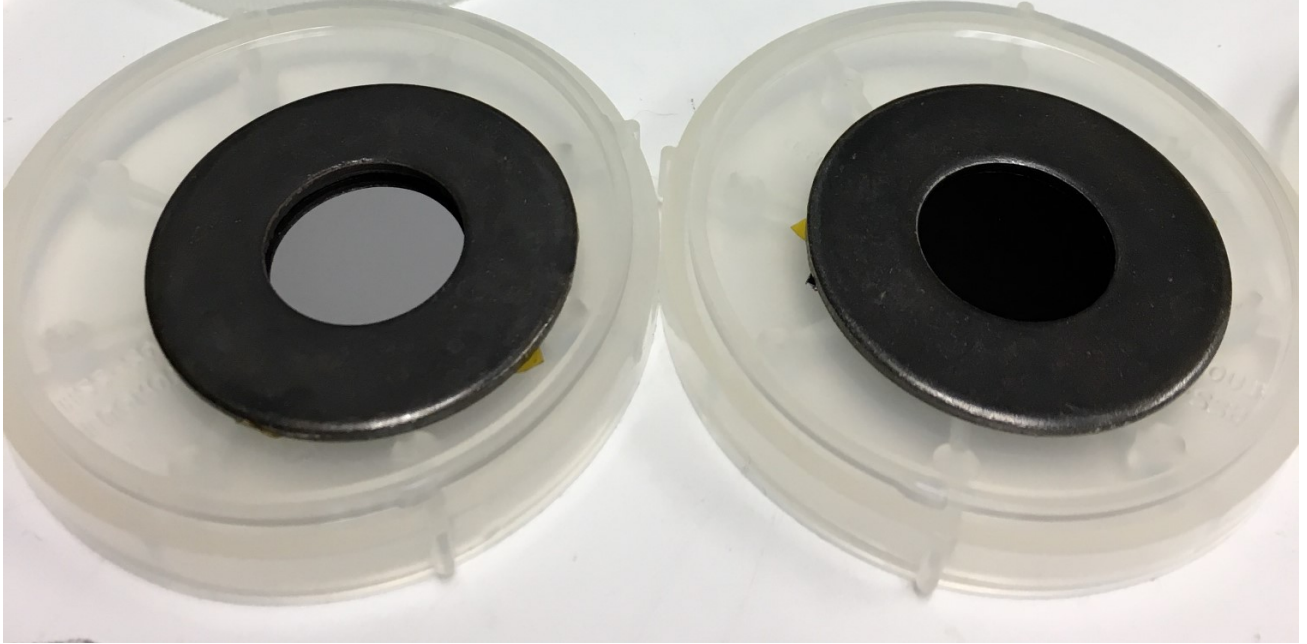


Figure 2. Photograph of untreated GaSb wafer (left) and etched “GaSb grass” wafer (right). Both wafers are mounted on metal washers with polyimide tape. The etched wafer is visibly and uniformly black, showing the antireflection of the coating and the absorption of visible light by GaSb.

### 3. EXPERIMENT

In our work, we seek to build on the  $\text{Cl}_2/\text{O}_2$  inductively coupled plasma (ICP) etch demonstrated by Lin *et al.*<sup>15</sup> In that work, the dimensions shown for the GaSb grass include widths from 74 to 121 nm and heights from 547 to 947 nm. We iteratively tuned the parameters of the etch, including ICP power, RF bias power, gas flow rates, and chamber pressure in order to achieve taller and wider grass, and to maximize density.

An example scanning electron microscope (SEM) image of the results is shown in Fig. 1. The results show grass of heights approximately 5 to 6  $\mu\text{m}$  and widths approximately 200 to 300 nm. (Note that the sample is viewed at  $30^\circ$  off-normal incidence, causing the heights to appear shorter by half).

The visual appearance of such a sample is shown in Fig. 2. This sample shows an untreated GaSb wafer next to an etched “GaSb grass” wafer. The etched wafer is uniformly black, showing the antireflection of the coating and the absorption of visible light by GaSb. Despite this, for wavelengths above the bandgap of GaSb the wafer will be transmissive (less free carrier absorption), so the coating can be treated there as an antireflective material and not an absorbing one.

### 4. RESULTS

In order to avoid backside reflection in the transmissive window of GaSb, we performed this etch on highly  $p^+$ -doped GaSb wafers. This increases free carrier absorption and nearly eliminates the transmissive window. We selected 3 sets of etch parameters and performed each etch on a single quarter of a 2-inch wafer, labeling the three samples 401, 402, and 403.

We measured the specular and diffuse reflectivity of the samples by Fourier Transform Infrared (FTIR) spectrometers, using an integrating sphere for diffuse reflectivity. Diffuse reflectivity was generally under 1% up to wavelengths of about 17  $\mu\text{m}$ . We plot total reflectivity (specular and diffuse reflectivity, summed) against wavelength in Fig. 3 for three typical etched samples as well as one untreated sample. Two FTIR systems were used, one from 200 nm to 2.5  $\mu\text{m}$ , and one from 2.5  $\mu\text{m}$  to 20  $\mu\text{m}$ . A discontinuity is visible at this point showing imperfect calibration of the two systems. For the best sample, sample 401, we demonstrate sub-10% reflectivity for wavelengths ranging from 200 nm to 12.2  $\mu\text{m}$ .

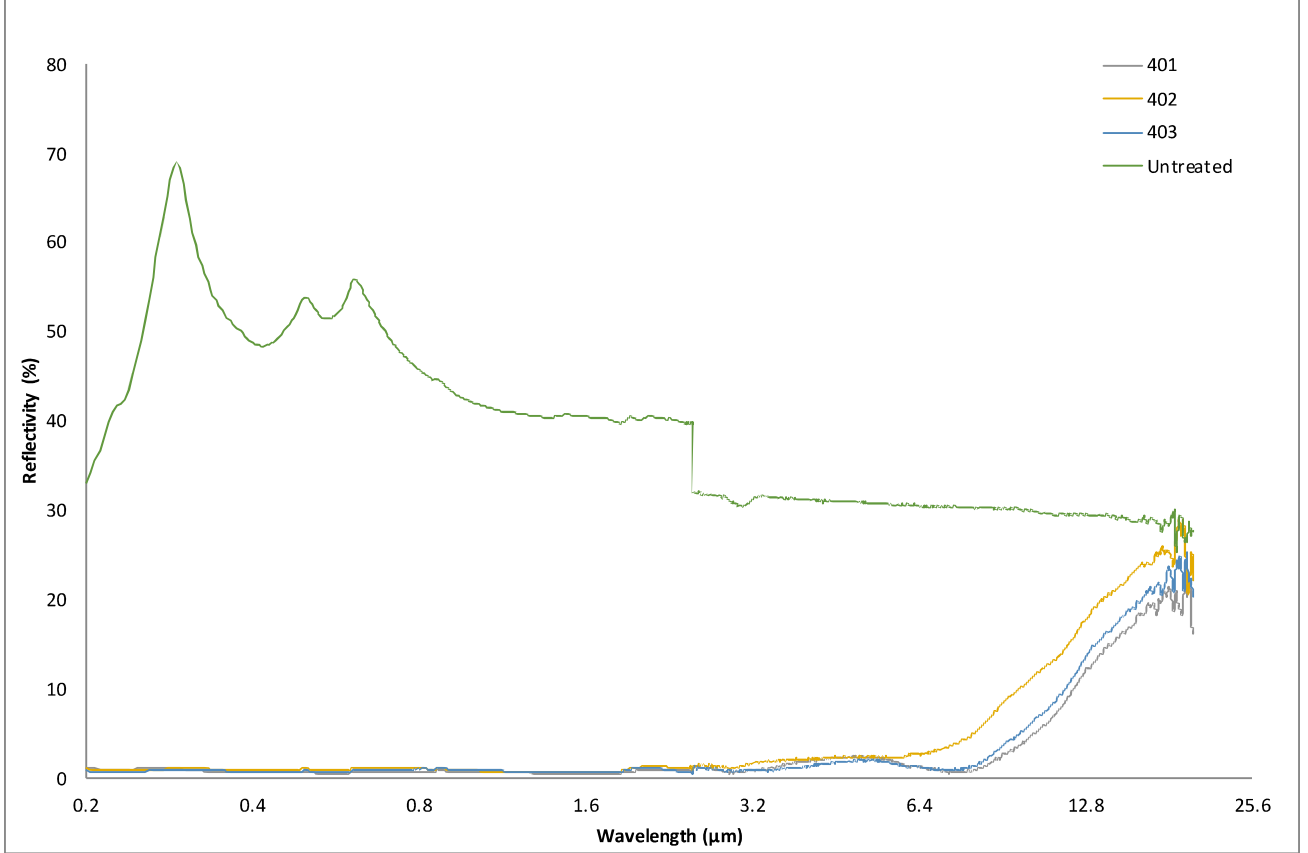


Figure 3. Total reflectivity vs. wavelength for 4 samples based on  $p^+$ -doped GaSb wafers to avoid backside reflection. One sample is untreated, while three (samples 401, 402, and 403) were etched using the described  $\text{Cl}_2/\text{O}_2$  inductively coupled plasma etch with different etch parameters.

We selected the second-best sample, 403, for characterization of specular reflectivity versus wavelength for several angles of incidence. This data was only taken for one FTIR spectrometer and is limited to the wavelength range from  $2.5\ \mu\text{m}$  to  $20\ \mu\text{m}$ . This data is shown in Fig. 4. This sample was measured at angles of  $0^\circ$ ,  $30^\circ$ ,  $38^\circ$ ,  $48^\circ$ ,  $58^\circ$ , and  $68^\circ$ . Even up to angles of incidence of  $58^\circ$ , a substantial part of the spectrum retains reflectivity below 10%.

## 5. CONCLUSION

In this work we have extended the  $\text{Cl}_2/\text{O}_2$  inductively coupled plasma etch technique originally described by Lin *et al.*<sup>15</sup> This creates a surface with extremely broadband antireflective properties. We have iteratively tuned the parameters of the etch, including ICP power, RF bias power, gas flow rates, and chamber pressure in order to achieve taller and wider grass, and to maximize density. This has allowed us to achieve grass with dimensions including heights approximately  $5$  to  $6\ \mu\text{m}$  and widths approximately  $200$  to  $300\ \text{nm}$ . We have also demonstrated sub-10% reflectivity for wavelengths ranging from  $200\ \text{nm}$  to  $12.2\ \mu\text{m}$  (nearly 6 octaves) and at angles of incidence up to  $58^\circ$ . Though antireflective GaSb grass has been explored before,<sup>11–17</sup> antireflection had previously been limited to a maximum wavelength of  $2.3\ \mu\text{m}$ .

This technique has potential for integration with GaSb-based infrared detectors, such as bulk InAsSb,<sup>1</sup> HOT-BIRDS,<sup>2,3</sup> and other nBn/XBn detectors<sup>4,5</sup> (a patent is pending regarding this integration). We have also performed some initial successful experiments integrating this GaSb grass with bulk InAsSb nBn detectors, however this is beyond the scope of the present work and will be covered in a forthcoming publication. This GaSb grass has the potential for substantial advantages over traditional dielectric coatings, including bandwidth, angle of incidence, delamination risk, and cost.

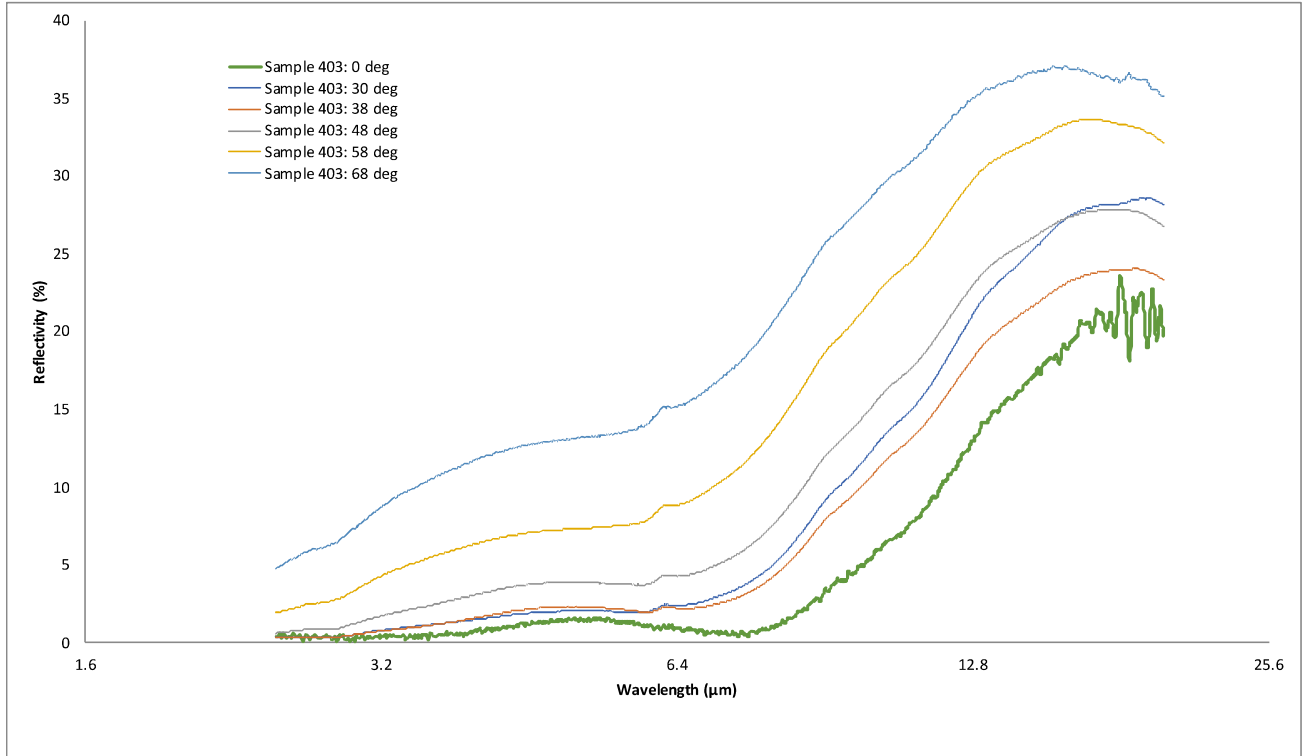


Figure 4. Specular reflectivity vs. wavelength for several angles of incidence on sample 403. Even up to angles of incidence of 58°, a substantial part of the spectrum retains reflectivity below 10%.

## ACKNOWLEDGMENTS

The research described in this publication was carried out at the Jet Propulsion Laboratory, California Institute of Technology, under a contract with the National Aeronautics and Space Administration. The authors thank Everett Fraser and Paul Pinsukanjana for assistance with wafers, Cory J. Hill for technical assistance, David Z. Ting for discussions, and Nicholas A. Heinz and Mark S. Anderson for assistance with the FTIR reflectivity measurements.

## REFERENCES

- [1] Klipstein, P., “XBn barrier photodetectors based on InAsSb with high operating temperatures,” *Optical Engineering* **50**, 061002 (Jun 2011).
- [2] Ting, D. Z., Soibel, A., Khoshakhlagh, A., Rafol, S. B., Keo, S. A., Höglund, L., Fisher, A. M., Luong, E. M., and Gunapala, S. D., “Mid-wavelength high operating temperature barrier infrared detector and focal plane array,” *Applied Physics Letters* **113**, 021101 (Jul 2018).
- [3] Soibel, A., Ting, D. Z., Rafol, S. B., Fisher, A. M., Keo, S. A., Khoshakhlagh, A., and Gunapala, S. D., “Mid-wavelength infrared InAsSb/InAs nBn detectors and FPAs with very low dark current density,” *Applied Physics Letters* **114**, 161103 (Apr 2019).
- [4] Maimon, S. and Wicks, G. W., “nBn detector, an infrared detector with reduced dark current and higher operating temperature,” *Applied Physics Letters* **89**, 151109 (Oct 2006).
- [5] Klipstein, P., “‘XBn’ barrier photodetectors for high sensitivity and high operating temperature infrared sensors,” in *[Infrared Technology and Applications XXXIV]*, Andresen, B. F., Fulop, G. F., and Norton, P. R., eds., SPIE (Apr 2008).
- [6] Jansen, H., de Boer, M., Legtenberg, R., and Elwenspoek, M., “The black silicon method: a universal method for determining the parameter setting of a fluorine-based reactive ion etcher in deep silicon trench etching with profile control,” *Journal of Micromechanics and Microengineering* **5**, 115–120 (Jun 1995).



- [7] Jansen, H., de Boer, M., Burger, J., Legtenberg, R., and Elwenspoek, M., “The black silicon method II: The effect of mask material and loading on the reactive ion etching of deep silicon trenches,” *Microelectronic Engineering* **27**, 475–480 (Feb 1995).
- [8] Liu, X., Coxon, P. R., Peters, M., Hoex, B., Cole, J. M., and Fray, D. J., “Black silicon: fabrication methods, properties and solar energy applications,” *Energy Environ. Sci.* **7**(10), 3223–3263 (2014).
- [9] Juntunen, M. A., Heinonen, J., Vähänissi, V., Repo, P., Valluru, D., and Savin, H., “Near-unity quantum efficiency of broadband black silicon photodiodes with an induced junction,” *Nature Photonics* **10**, 777–781 (Nov 2016).
- [10] Balasubramanian, K., Cady, E. J., Muller, R., Riggs, A. J. E., Ryan, D., White, V., Wilson, D., Yee, K., Echternach, P., Prada, C. M., Seo, B.-J., Shi, F., Fregoso, S., Metzman, J., and Wilson, R. C., “Systematic errors and defects in fabricated coronagraph masks and laboratory scale star-shade masks and their performance impact,” in [*Techniques and Instrumentation for Detection of Exoplanets VIII*], Shaklan, S., ed., SPIE (Sep 2017).
- [11] Knoedler, C. M. and Douglas C. LaTulipe, J., “Process for preparing a vertically differentiated transistor device,” (1986). US Patent 4759821A.
- [12] Swaminathan, K., Janardhanan, P., and Sulima, O., “Inductively coupled plasma etching of III–V antimonides in BCl<sub>3</sub>/SiCl<sub>4</sub> etch chemistry,” *Thin Solid Films* **516**, 8712–8716 (Oct 2008).
- [13] Kanamori, Y., ichi Kobayashi, K., Yugami, H., and Hane, K., “Subwavelength antireflection gratings for GaSb in visible and near-infrared wavelengths,” *Japanese Journal of Applied Physics* **42**, 4020–4023 (Jun 2003).
- [14] Min, W.-L., Betancourt, A. P., Jiang, P., and Jiang, B., “Bioinspired broadband antireflection coatings on GaSb,” *Applied Physics Letters* **92**, 141109 (Apr 2008).
- [15] Lin, T., Ramadurgam, S., Liao, C.-S., Zi, Y., and Yang, C., “Fabrication of sub-25 nm diameter GaSb nanopillar arrays by nanoscale self-mask effect,” *Nano Letters* **15**, 4993–5000 (Jul 2015).
- [16] Datta, D. P., Garg, S. K., Thakur, I., Satpati, B., Sahoo, P. K., Kanjilal, D., and Som, T., “Facile synthesis of a superhydrophobic and colossal broadband antireflective nanoporous GaSb surface,” *RSC Advances* **6**(54), 48919–48926 (2016).
- [17] Datta, D. P. and Som, T., “Nanoporosity-induced superhydrophobicity and large antireflection in InSb,” *Applied Physics Letters* **108**, 191603 (May 2016).
- [18] Deinega, A., Valuev, I., Potapkin, B., and Lozovik, Y., “Minimizing light reflection from dielectric textured surfaces,” *Journal of the Optical Society of America A* **28**, 770 (Apr 2011).